Long-wavelength phonons in $TlSbS_2$. II. Raman-active modes under hydrostatic pressure

P. Rouquette, B. Gil, and J. Camassel
Groupe d'Etude des Semiconducteurs, Université des Sciences et Techniques du Langeudoc, F-34060 Montpellier CEDEX, France

J. Pascual
Department de Física–ICMAB, (C.S.I.C.), Universitat Autònoma de Barcelona, S-08193 Bellaterra, Spain
(Received 10 June 1988; revised manuscript received 20 September 1988)

We report the evolution of the first-order Raman modes of the layered semiconductor $TlSbS_2$ with hydrostatic pressure applied up to 10 kbar. All the modes experience a blue shift, except the mode at 286 cm^{-1}, whose insensitivity to pressure shows it to be governed by stretching of Sb-S diatomic chains in the layer. An axially symmetric short-range potential between nearest neighbors has been constructed to account for the full Raman spectrum.

I. INTRODUCTION

High-pressure experiments have proved to be one of the most powerful tools for investigating new phases in solids. Of particular interest are the large number of investigations devoted to study structural phases in tetrahedrally coordinated network semiconductors, like Si,[1] where parallel progress in the thoeretical knowledge of this *simple* system[2] has made pressure effects to be one of the most interesting subjects we have at present.

Among the physical properties of materials, the investigation of forces which hold bound atoms in crystals by means of Raman experiments has been one of the most benefitted with the advent of improved diamond-anvil cell apparatus. The reason is clear, three-dimensional network crystals are scarcely compressible so that hydrostatic pressures of some kilobars does not produce appreciable changes in the Raman spectrum.[3]

This is not the case for molecular crystals, where great disparity between intermolecular and intramolecular distances make them to be much more sensitive to a hydrostatic stress perturbation and considerable information, mainly concerning the intermolecular interactions, can be obtained in the low pressure regime.[3]

There are three major features which characterize the Raman and pressure Raman spectra of molecular solids and differentiate them from network crystals.

(1) To a greater molecular character of the solid corresponds a larger separation between intermolecular and intramolecular modes in the Raman spectrum. Crystalline α-As_4S_4 is a beautiful example in which the three ranges of energies corresponding to intramolecular bond-stretching modes and intramolecular bond-bending modes of octaatomic molecules and intermolecular modes determined primarily by S-S contacts are clearly separated.[4].

Moreover, the molecular character of the solid manifests also by the competition between molecular and crystal symmetry in photon-photon selection rules. An example is crystalline As_2S_3 where polarized Raman experiments have demonstrated the dominance of the layer symmetry over the crystal symmetry.[5]

(2) Modest pressures produce large effects in molecular crystals. The notable difference in bond lengths produces a hierarchy of force constants which gives rise to a corresponding selective action of hydrostatic stress stiffening the softest bonds in the crystal. The decreasing ratio of intermolecular-intramolecular force constants induced by pressure results in a progressive loss of the molecular character of the crystal. This is probed by the fast tendency of intermolecular modes to approach the intramolecular region in the Raman spectrum. It is not unusual to find, for intermolecular modes, energy shifts of 100% or more upon the application of stresses of a few tens of kilobars, see, for example, the evolution of the external modes of crystalline P_4S_3, a zero-dimensional network crystal.[6]

Moreover, the large number of atoms that molecular crystals normally have per unit cell gives rise to a large number of Raman-active phonons. This richness makes it difficult to identify individual modes, however it reveals global aspects of the response to pressure. For example, from the correlation between pressure sensitivity and phonon frequency, one can obtain an estimate of the hierarchy of forces.[7] This is reflected in the drastic departure of phonons from Grüneisen scaling, a concept which works very well for rigid three-dimensional networks but which has been shown to fail to explain the behavior of molecular crystals, where the Grüneisen parameter varies systematically over the phonon spectrum by 1–3 orders of magnitude.[4,7]

(3) Because intermolecular modes are so sensitive to pressure, hydrostatic stresses can help to resolve near-degenerate modes by enhancing their splitting,[3] a technique which is complementary to the widespread use of low temperature to enhance resolution. The intralayer triplet of As_2S_3 near 360 cm^{-1} is an example,[8] where pressures of about 30 kbar give much better resolution than cooling down the crystal to 15 K.

In spite of the fact that the previous features are characteristic of a large variety of molecular crystals, the simple and often-observed behavior embodied by Zallen's

law[4,7] which predicts, for modes beyond the external-mode regime, an approximate inverse-square correlation between the mode Grüneisen parameter and the mode frequency, $\gamma_i \sim \nu_i^{-2}$, is not always followed. This presumably occurs for materials which present a complex hierarchy of force constants instead of a clear division into intramolecular and intermolecular bonds, like the thallium chalcogenides $TlGaX_2$ (X=S, Se) for which a high-pressure Raman study[9] has shown that log-log plots of pressure-induced frequency shifts versus the initial frequencies have slopes different from -2, the value expected from Zallen's analysis.

In order to give more insight into the problem of the response of phonons to pressure in molecular crystals, we report in this paper the results of an extensive experimental investigation on the effect of pressure upon Raman-active modes of $TlSbS_2$. This is a layer compound semiconductor with similar chemical formula, but a completely different crystal structure, than $TlGaX_2$. Its elementary cell consists of four molecular units disposed in two sheets forming the layer. Examination of the structure shows that in a given sheet the atoms are arranged in couples of alternate linear Tl-S and Sb-S chains extending in the b direction while viewed from a results in chains of Tl-S-Sb-S series of atoms.[10] This strong anisotropy of the structure, not only perpendicular to the layer but also in the layer along the two chain directions, is reflected in the anisotropic character of the electronic properties[11] and lattice dynamics.[12-14] Since there is only one layer per unit cell, rigid layer modes correspond to zone-boundary wave vectors and are absent in the first-order Raman spectrum. The same comment applies to Davydov splittings, which, in this case, are nothing but the measure of the dispersion of the optical branches along c and cannot be determined by first-order Raman spectroscopy.

II. EXPERIMENTAL DETAILS

Hydrostatic pressure was applied, up to 10 kbar, using a pressure cell which has been published elsewhere.[15] All of the experiments were taken at room temperature with cleaved faces parallel to the layer plane and the laser beam impinging, at normal incidence, upon the cleaved face, and with the collected scattered radiation in the backscattering configuration. The Raman spectra were taken with polarized incident and scattered light, in order to have the $c(aa)c$ and $c(bb)c$ configurations. The reasons for analyzing only these two configurations are that all the modes have been identified in those configurations and, although some modes are stronger in other configurations (see Ref. 12), the good signal-to-noise ratio we get in backscattering experiments performed normal to the freshly cleaved samples as compared with experiments performed on polished surfaces which contain the c axis, assures good detection of all the observed Raman modes including those with a meager intensity.

Because $TlSbS_2$ has a large number of Raman-active modes,[12,14] a larger number of mode-frequency pressure coefficients have been determined in this study. Typical near-resonance Raman spectra for $c(aa)c$ and $c(bb)c$ configurations, at room temperature, obtained by means of the 7525-Å line of the krypton laser with a power of about 200 mW, and taken with conventional Raman set-up,[12] are displayed in Fig. 1. A detailed study of the most important features in the Raman spectrum has been given in Ref. 14 (henceforth called paper I), in terms of a simple molecular chain model which has also proved to be very successful in explaining the infrared experiments.[13]

III. EXPERIMENTAL RESULTS

We have followed the evolution of 15 modes in the $c(aa)c$ configuration and 10 modes in the $c(bb)c$ configuration. In our previous study at room temperature,[12] we identified, respectively, 14 and 13 modes.[16] The new mode at 248 cm^{-1} found in the $c(aa)c$ configuration depends strongly on the quality of the sample. It is a weak mode which for most of the samples smears out in the broad scattering of the phonon at 227 cm^{-1}. For the $c(bb)c$ spectrum, the weak intensity and large linewidth of modes at 175 and 200 cm^{-1} prevented measurement of their pressure shift.

The correspondence between all the modes found in both configurations is very good except for the doublet at 285.5–288 cm^{-1}. Presumably this large shift is due to the different scattering efficiency of the two partner modes which take part in this broad line. As was shown in paper I, at 80 K the intensity of both modes is almost

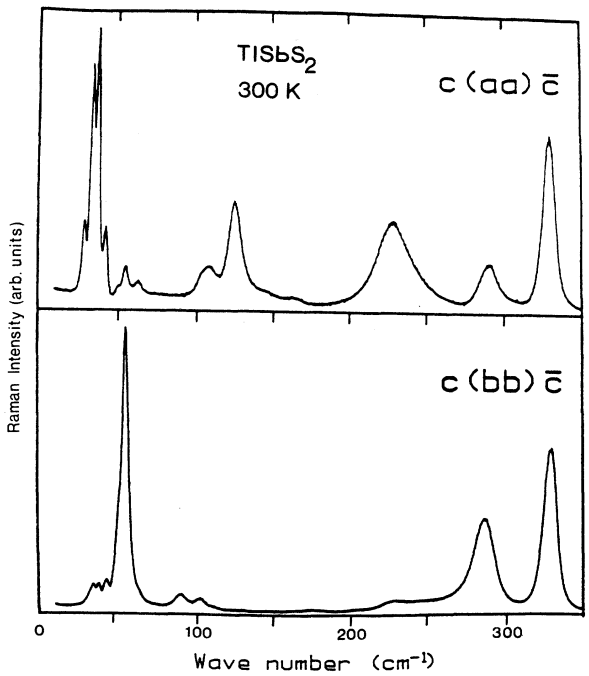

FIG. 1. First-order Raman spectrum of $TlSbS_2$, obtained at room temperature on the large face of a single crystal cleaved perpendicular to c. The spectra have been taken in the back scattering configuration using the 7525-Å line of krypton-ion laser as the exciting radiation.

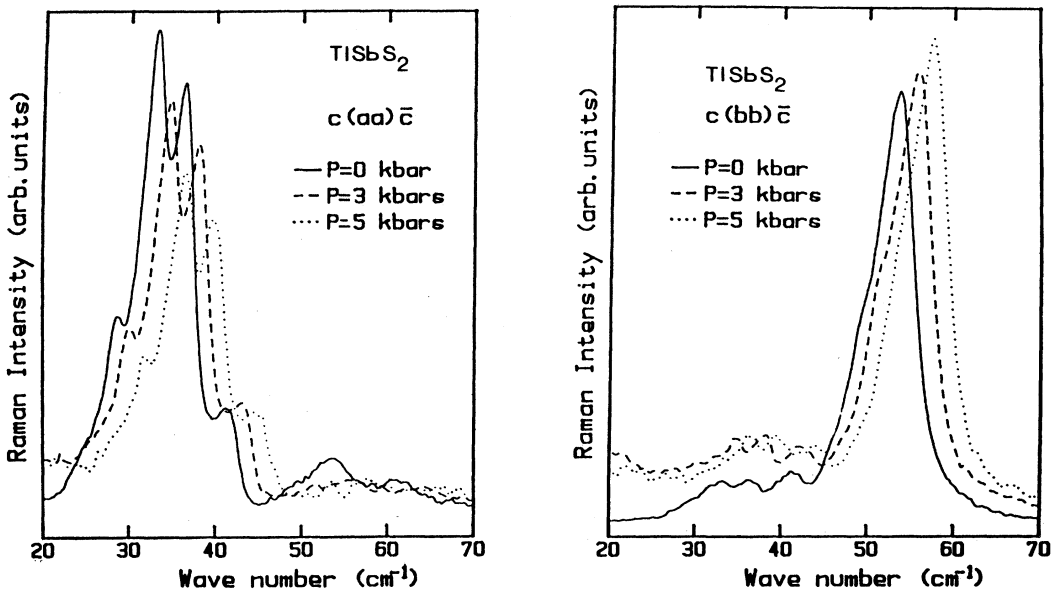

FIG. 2. Pressure shift of Raman active modes below 70 cm^{-1} for the two configurations discussed in the text. These experimental spectra are representative of the evolution of the energy with pressure for all the modes in the spectrum.

the same in the $c(aa)c$ configuration while the lower mode has an intensity of twice or more than the upper mode in the $c(bb)c$ configuration. If the relative scattering efficiency does not change very much from 80 K to room temperature, we expect that the partner modes smear out into an unresolved band whose maximum is shifted for $c(bb)c$ to lower energy. Since from the molecular chain model presented in paper I, the two partner modes arise from the same strong Sb—S bond-stretching interaction along the b direction, we expect that the two peaks, 3 cm^{-1} apart, found in the two configurations, to shift in the same way.

Figure 2 shows detailed Raman spectra for the low-frequency modes at ambient pressure and at 3 and 5 kbar. This figure is representative of what happens in the rest of the Raman spectrum. All modes experience a blue shift with pressure with a rate ranging roughly between 0.9 and 0.3 cm^{-1}/kbar, except for the mode at $\sim$286 cm^{-1} which is almost insensitive to the external perturbation. The set of slopes of frequency and relative frequency shifts with pressure are listed in Table I. The modes found in both configurations have the same measured slopes, within experimental error. Larger difference between mean values occur for the modes at 227, 53.5, and 49.5 cm^{-1}. From Fig. 1 we see that the mode at 227 cm^{-1} is very weak in the $c(bb)c$ configuration and shows a relatively large linewidth. Since the experimental error is smaller for the $c(aa)c$ configuration where it is strongly allowed, we will take for this mode the mean value measured in this last configuration. Concerning the modes at 53.5 and 49.5 cm^{-1}, the first one is the strongest phonon observed in $c(bb)c$ configuration where one can easily follow its evolution with pressure. On the contrary, in the $c(aa)c$ configuration it is quite weak and it tends to diminish in intensity with hydrostatic stress to a level lower than the one of the close mode at 49.5 cm^{-1}. Preliminary studies on resonant Raman scattering[17] at 80 K show a strong Raman line dependence of the intensity ratio between the two modes in $c(aa)c$ configuration. Both the bad resolution of the two modes at room temperature and the different changes in intensity with pressure can explain the difference between the mean values obtained in the $c(aa)c$ and $c(bb)c$ configurations. Pressure opens the energy gap and, for a given Raman line, it must have an effect upon the intensities of modes roughly equivalent to receding from resonance by changing the incident laser light in a zero pressure experiment. These considerations support the assignment of the mean values measured in the allowed $c(bb)c$ configuration for the two modes.

Overall pressure-induced changes are most easily seen by plotting the Raman frequencies versus pressure as shown in Fig. 3. The simplest case for discussion is $c(bb)\bar{c}$ where a clear gap is open between high-frequency modes above 200 cm^{-1} which upshift slowly with pressure, and low-frequency modes below 100 cm^{-1}, which experience a rapid relative shift. Above 200 cm^{-1}, the Raman and infrared peaks found in the experiments can be assigned to intramolecular SbS or SbS_2 vibrations, depending on the mode polarization[12,13] and because of the molecular character of the modes one expects small shifts with pressure. This is reflected in Table I, where very sluggish changes are measured for the relative shift of "internal" modes. The influence of pressure upon these modes is so weak that no additional information like an expected splitting of the two Raman modes around 328 cm^{-1} or the other two modes at $\sim$287 cm^{-1} can be obtained. The insensitivity of these high-energy modes is due to the hardness of the short Sb—S bonds along c (d=2.41 Å) and b (d=2.45 Å). Assuming all force con-

stants to vary like r^{-n}, Zallen predicts[7] the ratio of Grüneisen parameters of two internal modes to be

$$\gamma_i/\gamma_{i'} \sim K_{i'}/K_i = (r_{i'}/r_i)^{-n} .$$

Taking $n=7$, the quotient for the Grüneisens of the modes associated with molecular vibrations along a ($\nu_a = 227$ cm^{-1} and $d=2.75$ Å) and the hardest stretching vibrations along b or c ($\nu_b = 288$ cm^{-1}, $\nu_c = 328$ cm^{-1}, and $d \sim 2.45$ Å) is 0.45, against the experimental results of 0.7 and 0.4 for ν_c and ν_b, respectively.

A different situation occurs for the two partner modes at 248 and 227 cm^{-1}, which are associated with stretching vibrations of SbS_2 molecules along a. The large splitting of 21 cm^{-1} between the two peaks is due to the occurrence of two types of SbS_2 molecules, one having almost equal Sb-S arms ($d \sim 2.75$ Å) while the other showing completely asymmetric Sb-S distances (2.96 and 2.60 Å). These bonds, longer than the typical 2.45-Å value for b and c bonds, are more sensitive to the external perturbation. In particular, the mode at 227 cm^{-1} shows a relative shift almost three times greater than the mode at 248 cm^{-1}. From its Raman efficiency, we associate the lower mode to the stretching vibration of the asymmetric molecular SbS_2 unit. According to this model and Zallen's prediction that pressure stiffens the softest bonds, the mode at 248 cm^{-1} would experience a weaker shift with pressure than the strong Raman-active mode at 227 cm^{-1} because the much longer Sb-S arm in the asymmetric molecule must contract faster. The experimental

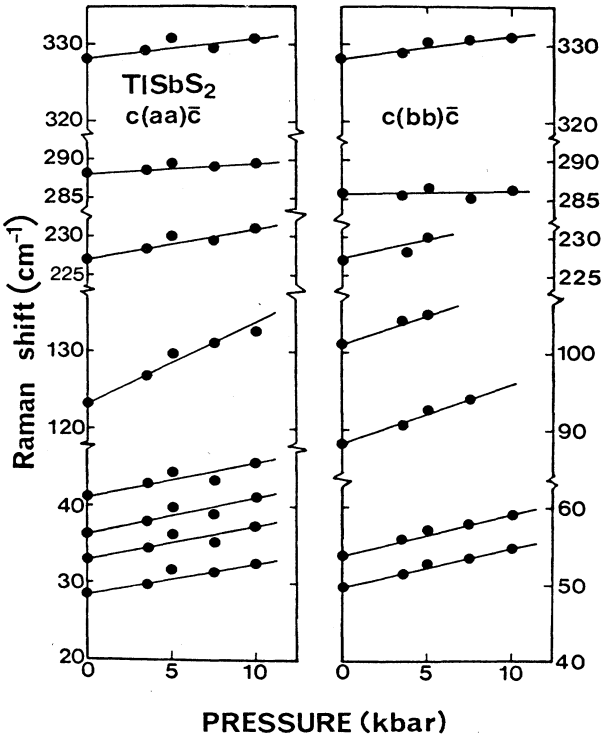

FIG. 3. Raman shift with pressure for the modes followed in $c(aa)c$ and $c(bb)c$ configurations. Notice the different sensitivity to the external perturbation of molecular and network modes.

TABLE I. Pressure coefficients of Raman-active modes of $TlSbS_2$. Estimated experimental error for the relative pressure shift range between 10% for modes below 130 cm^{-1} and 30% for Raman modes above 200 cm^{-1}.

Phonon energy	Relative shift at 10 kbar	Pressure shift $\frac{d\nu}{dP}$ (cm^{-1}/kbar)		Relative pressure shift $\frac{1}{\nu}\frac{d\nu}{dP}$ (10^{-3} kbar^{-1})	
ν (cm^{-1})	$\frac{d\nu}{\nu}$ (%)	$c(aa)\bar{c}$	$c(bb)\bar{c}$	$c(aa)\bar{c}$	$c(bb)\bar{c}$
28.5	13	0.38		13.2	
33	13	0.40	0.45	12.2	13.5
36.5	13	0.45	0.47	12.2	13.0
41.5	10	0.41	0.41	10.5	9.8
49.5	10	0.57	0.51	11.5	10.3
53.5	10	0.70	0.54	13.0	10.0
61.5	8	0.51		8.6	
88	9		0.80		9.1
101	8		0.85		8.5
106	7	0.75		7.1	
123	8	0.97		7.8	
144	5	0.71		5.0	
163	3	0.57		3.5	
227	2	0.39	0.50	1.8	2.2
248	0.5	0.14		0.6	
285.5	0.1		0.03		0.1
288	0.4	0.12		0.4	
328	0.9	0.25	0.32	0.7	1

reltive shift with the pressure for the upper and lower modes are, respectively (see Table I) 0.6 and 1.8 in units of 10^{-3}/kbar. Taking Zallen's prediction for the Grüneisen ratio one calculates quotient of 1.8 in fairly good agreement with the experimental value of 3.0.

This simple model explains qualitatively why the weak $A_g(a)$ mode shifts less than the strong $A_g(a)$ mode and why $A_g(a)$ modes are more sensitive to stress than $A_g(b)$ or $A_g(c)$ modes, but cannot account for the different behavior of these two last modes where the interatomic Sb-S distance is much the same. Indeed, the system is much more complex than we have thought. Although the short Sb-S distances give rise to strong force constants which account for the energy of the modes, Tl atoms can play a nonnegligible role when pressure is applied. So, for $A_g(a)$ modes the S-Sb-S triatomic molecules are coupled along a linear chain by bridges of Tl atoms, or, along c, there is an interlayer mismatch between Sb-S molecules which couple Sb-S and Tl-S chains.[10] On the contrary, along b, the dimerized Sb-S molecules are aligned along chains with very weak direct intermolecular couplings. One can say that the dimerized molecules along b are those which best retain molecular character and, as a consequence, are least influenced by the external perturbation. In order to test the validity of these assumptions we will develop in the next paragraph a more realistic model to calculate the eigenenergies and eigenstates of phonons at the center of the Brillouin zone.

The necessity to include Tl—S and Sb—S bonds as well in calculations is also clear from the different scaling of experimental Grüneisen parameters for low- and high-energy modes. In paper I we showed that molecular Sb-S interactions in the coupled dimerized chains along b gave a good account of the experimental results: the doublet at ~ 287 cm^{-1} and the low mode at 53.5 cm^{-1}. But in this crude model all frequencies scale proportional to the Sb—S bond stretching, thus the calculated Grüneisen parameters would be the same for the three modes. In fact, the chain model developed in paper I for the three main directions is built from stretching and bending force constants of short Sb-S interactions and although it gives the essential contribution for high-energy modes, longer and softer bonds must play an important role when modes are perturbed by the applied pressure. If one performs a Zallen plot[4] of the correlation between pressure sensitivity and phon frequency for $TlSbS_2$ [see Fig. 4(a)], one finds a similar behavior to the one which occurs in molecular solids.[3] The small frequency dependence of the Grüneisen scaling for phonons below 100 cm^{-1} reflects the fact that there is not a principal interaction which governs the pressure shift. In some respects, $TlSbS_2$ is an intermediate compound between molecular solids where a net separation exists between internal and external modes and complex solids like $TlGaX_2$ chalcogenides where there is a hierarchy of force constants.[9]

IV. DISCUSSION

$TlSbS_2$ has some peculiarities which differentiates it from "normal" low-dimensional crystals. First, this compound contains only *one* layer per unit cell and rigid layer modes and Davydov multiplets arising from the coupling

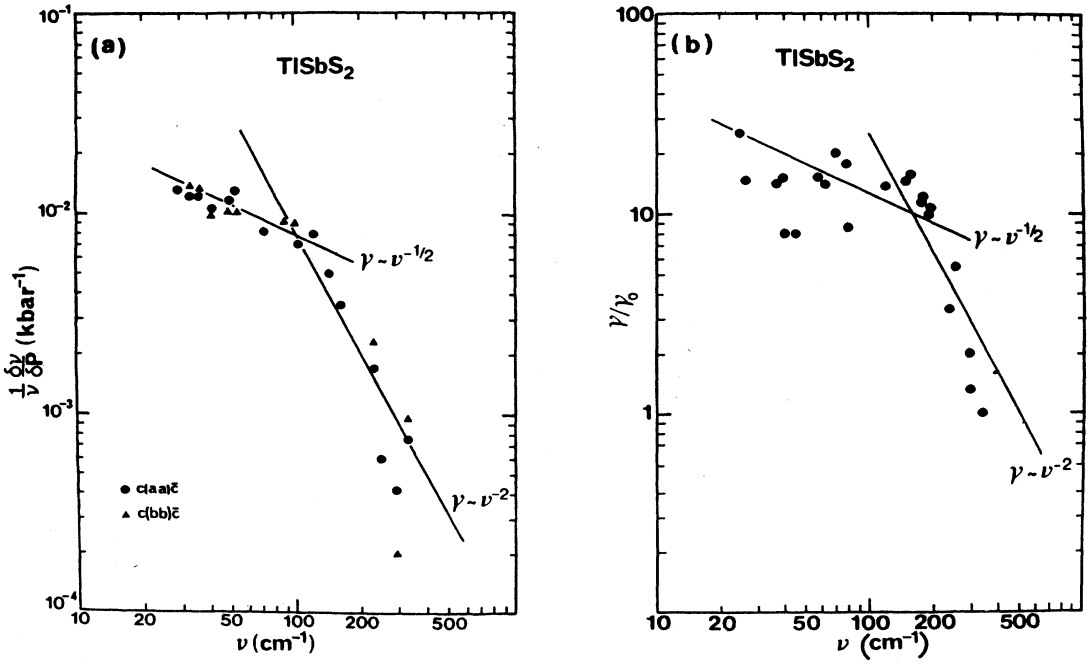

FIG. 4. (a) Relative Raman shift with pressure against the energy of the modes. The modes above 200 cm^{-1} follow Zallen's law. By contrast, the dependence of the relative shift with pressure for low-energy modes shows that a hierarchy of forces exists in $TlSbS_2$. (b) Calculated Grüneisen parameter for the 24 Raman active modes. Because the compressibility of $TlSbS_2$ is unknown, we report the relative Grüneisen parameter normalized with respect to the highest energy modes.

of nonequivalent layers in the crystal cannot be found in a first-order Raman scattering experiment. Only occasionally second-order Raman experiments or neutron-diffraction measurements of the dispersion of the acoustic and optic branches along c can give a measure of the interlayer coupling. Second, $TlSbS_2$ has, in the layer, a chainlike structure governed by short Sb-S interactions and more relaxed Tl—S bonds where no identical entities take part in the unit cell: thus, one cannot distinguish between interchain and intrachain interactions. This makes more difficult the analysis of data because there is not a clear cut between internal and external modes. The great disparity of interatomic distances which occurs in a layer, ranging from 2.41 Å for Sb-S interactions along c to 3.37 Å for Tl—S bonds along a, suggests a hierarchy of forces in the layer which provides a basis for discussing the experimental results.

The calculations performed in paper I and in the last paragraph were inspired by a very schematic view of the layer but nevertheless they show the outstanding features of the Raman spectrum. A more detailed treatment of the dynamical matrix, including short-range interactions, will be attempted here. Keeping simplicity as far as possible, the model lies in the following reasonable assumptions.

(i) Reference 10 show that the angles between the two Sb—S (Tl—S) bonds which meet at a common Sb (Tl) atom are close to 90°. Thus, for simplicity we take the orthorhombic analog of the real structure as shown in Fig. 7 of paper I. This symmetric model corresponds to the C_{2h} point group and the $16\times3=48$ normal modes of vibration at $k=0$ decouple into

$$\Gamma(C_{2h})=12A_g+12B_g+12A_u+12B_u\ .$$

The 24 inversion-invariant modes, $12A_g+12B_g$, are Raman active and become the 24 Raman active modes, all having the same symmetry in the real structure. Since the crystal unit cell contains *only one* layer, the symmetry of the crystal is also C_{2h}.

(ii) Because there is only one layer per unit cell and the ratio between intralayer and interlayer distances is quite small, the interlayer interactions serve only to weakly shift the intralayer energy of modes and cannot induce rigid-layer modes or Davydov splittings, so we can neglect their influence and calculate the phonon energies of the layer and compare them with experimental results.

(iii) Only short-range interactions between nearest neighbors will be taken into account.

A first choice of the bond stretching and axially symmetric bond-bending force constants in the "orthorhombic" structure have been taken to fit the experimental Raman results of the molecular modes above 200 cm^{-1} and the phonon energies in the range of 160–180 cm^{-1}, where Tl-S interactions participate. For the axilally symmetric bond-bending force constants, we have taken a value roughly 1 order-of-magnitude lower than the corresponding bond-stretching force constant and with the same sign. A further slight modification of bending constants has been done in order to fit the experimental doublets at 285.5–288 cm^{-1} and 227–248 cm^{-1}. By contrast, it has not been possible to reproduce the splitting of the upper modes at ~328 cm^{-1} without strongly disturbing the fit of other lower modes. Table II collects all bond lengths and force constants used in our calculations. The application of the four symmetry operations of the orthorhombic layer, $\{E|0\}$, $\{I|0\}$, $\{C_{2z}|2a\mathbf{i}+a\mathbf{j}\}$ and $\{\sigma_h|2a\mathbf{i}+a\mathbf{j}\}$ gives a set of symmetrized coordinates which provides a basis set for describing the eigenstates. These symmetrized coordinates can be taken along the "crystallographic" directions and the 48×48 dynamical matrix can be decoupled into twelve 4×4 matrices, with four 4×4 matrices for each direction of polarization.

The 48 phonon energies calculated by solving the matrices are summarized in Table III. Although our model is the simplest one which couples all atoms in the layer, the calculations reproduce fairly well the experimental results. An examination of the eigenstates associated with each of the 48 phonons[17] show that over 200 cm^{-1}, only Sb-S vibrations participate. Also, for each quarter (two Raman active modes and two ir active modes), the even (odd) coupling of even and odd molecular modes give the corresponding Raman (infrared) active modes.

Figure 4(b) plots the results of the calculation of the relative Grüneisen parameters, normalized with respect to the highest-frequency mode, obtained from a simultaneous variation of bond stretching and bond-bending force constants. The results are in fairly good agreement, in view of the crudeness of the model, with the experimental data of Fig. 4(a).

V. CONCLUSIONS

We have followed the evolution with pressure, up to 10 kbar, of 15 modes in the $c(aa)c$ configuration and 10 modes in the $c(bb)c$ configuration. All the modes experience a blue shift with rates ranging between 0.9 and 0.3 cm^{-1}/kbar. The only exception is the mode at 285.5 cm^{-1} which remains insensitive to pressure; this has permitted us to identify this mode with Sb-S vibrations along the b axis.

Because the simple molecular model cannot explain

TABLE II. Interatomic distances and force constants used in the theoretical calculation of the 48 zone-center modes of $TlSbS_2$. The subscript labels for the atoms correspond to their position in the unit cell (see Fig. 6 in Ref. 14).

Bond	Bond length (Å)	Bond-stretching force constants (10^5 dyn/cm)	Bond-bending force constants (10^5 dyn/cm)
Sb_3—$S_{4'}$	2.420	1.610	0.260
Sb_3—S_7	2.455	1.160	0.188
Sb_3—S_2	2.655	0.665	0.075
Sb_3—S_4	2.885	0.235	0.034
Sb_3—S_7	3.700	0.023	0.003
Tl_1—S_2	3.340	0.070	0.011
Tl_1—S_4	3.145	0.128	0.021
Tl_1—S_5	3.065	0.165	0.027
Tl_1—S_5	3.203	0.106	0.018
Tl_1—$S_{2'}$	3.115	0.140	0.023

TABLE III. Comparison between theoretical zone-center modes of $TlSbS_2$ calculated in this work and experimental Raman and infrared-active modes.

Raman modes			Infrared modes	
ν (cm^{-1}) 300 K[a]	ν (cm^{-1}) 77 K[b]	ν (cm^{-1}) Theory[c]	ν (cm^{-1}) 300 K[d]	ν (cm^{-1}) Theory[c]
29	30.2	26		
	31.5	27		
34	35.2	37		
37	38.5	39	29	34
	43	42	33	35
42	44	46	40	43
49.5	51.5	58	56.5	56
54.5	56.5	62	60	59
62.5	65	70	66	59
88	91	78	101	64
101	104	81	109	76
107	109	119	116	92
	112.5	151	130	152
125	129	156	145	156
145	149	181	156	183
165	166.5	182	167	183
175	178	188	182	195
200	202	189	190	200
230	229.5	234	238	237
250	250	250	255	253
287	290.5	289	287	289
290	294.5	294	296	295
329	330	335	335	337
	334	335	341	337

[a]Reference 12.
[b]Reference 14.
[c]This work.
[d]Reference 13.

satisfactorily the experimental results we have built a more complex dynamical matrix in terms of axially symmetric force constants between nearest neighbors, calculated according to a simple Born's law. $TlSbS_2$ does not follow an exact Zallen's law principally for the modes of energy lower than 200 cm^{-1}. Accordingly, we classify $TlSbS_2$ as a layer semiconductor intermediate between those which are governed by essentially two kind of bonds and those in which a complicated hierarchy of force constants exist.

[1]T. H. Lin, W. Y. Dong, K. J. Dunn, C. N. J. Wagner, and F. P. Bundy, Phys. Rev. B **33**, 7820 (1986), and references therein.
[2]K. J. Chang and M. L. Cohen, Phys. Rev. B **30**, 5376 (1984).
[3]B. A. Weinstein and R. Zallen, in *Light Scattering in Solids IV*, edited by M. Cardona and G. Guntherodt (Springer, Berlin, 1984).
[4]R. Zallen and M. L. Slade, Phys. Rev. B **18**, 5775 (1978).
[5]R. Zallen, M. L. Slade, and A. T. Ward, Phys. Rev. B **3**, 4257 (1971).
[6]T. Chattopadhyay, C. Carlone, A. Jayaraman, and H. G. v. Schnering, Phys. Rev. B **23**, 2471 (1981).
[7]R. Zallen, Phys. Rev. B **9**, 4485 (1974).
[8]J. M. Besson, J. Cernogora, and R. Zallen, Phys. Rev. B **22**, 3866 (1980).
[9]W. Henkel, H. D. Hochheimer, C. Carlone, A. Werner, S. Ves, and H. G. v. Schnering, Phys. Rev. B **26**, 3211 (1982).
[10]M. Rey, J. C. Jumas, J. Oliver-Fourcade, and E. Philippot, Acta Cryst. C **39**, 971 (1983).
[11]P. Rouquette, J. Allegre, B. Gil, J. Camassel, H. Mathieu, A. Ibanez, and J. C. Jumas, Phys. Rev. B **33**, 4114 (1986).
[12]P. Rouquette, J. Camassel, G. Bastide, L. Martin, J. Oliver-Fourcade, and E. Philippot, Solid State Commun. **60**, 709 (1986).
[13]A. Goullet, P. Rouquette, J. Camassel, J. Pascual, and J. C. Jumas, Solid State Commun. **62**, 187 (1987).
[14]P. Rouquette, J. Allegre, J. Camassel, and J. Pascual, Phys. Rev. B **38**, 12 470 (1988).
[15]B. Gil, M. Baj, J. Camassel, H. Mathieu, C. Benoit a la Guillaume, N. Mestres, and J. Pascual, Phys. Rev. B **29**, 3398 (1984).
[16]In Table I of Ref. 12 there are only 12 modes in $A_g(b^2)$ configuration. We forget to put the mode at 33.1 cm^{-1}, clearly shown in the inset of Fig. 2(b).
[17]P. Rouquette, Ph.D. thesis, Université des Sciences et Techniques du Languedoc, 1987 (unpublished).